International Journal of Mathematics And its Applications
Volume 4, Issue 3–B (2016), 51–59.
ISSN: 2347-1557
Available Online: http://ijmaa.in/

International Journal of Mathematics And its Applications

# Unsteady Hydromagnetic Gas Flow Along an Inclined Plane With Indirect Natural Convection in the Presence of Thermal Radiation

**Research Article**

**B.Prabhakar Reddy**[1,2,*]

1 Department of Mathematics, The University of Dodoma, P. Box. No. 259, Dodoma, Tanzania.

2 Department of Mathematics, Geethanjali College of Engineering and Technology, Cheeryal (V), Keesara (M), Telangana, India.

**Abstract:** The Numerical solution of an unsteady gravity-driven thermal convection flow of a viscous incompressible, electrically-conducting, absorbing-emitting, optically-thick gray gas along an inclined plane in the presence of thermal radiation and a transverse magnetic field effects are carried out. The Rosseland diffusion flux model is employed to simulate thermal radiation effects. The momentum and energy conservation equations are non-dimensionalzed and solved by using Ritz finite element method. The effects of Prandtl number ($P_r$), Boltzmann-Rosseland radiation parameter ($K_1$), Hartmann number squared ($M^2$), porosity parameter ($K$), Grashof number ($G_r$), time parameter $t$ and plate inclination ($a$) on the velocity ($u$) and temperature ($\theta$) distributions are studied. Results obtained show that a decrease in the velocity and temperature occurs when Prandtl number and Hartmann number square root are increased. The velocity and temperature enhanced as Boltzmann-Rosseland radiation parameter and Grashof number are increased.

**Keywords:** Boltzmann-Rosseland radiation parameter, free convection, transient flow, gravity, thermal radiation.



## 1. Introduction

MHD radiative flows occurs in many areas of technology and applied physics including oxide melt materials processing, astrophysical fluid dynamics, plasma flows switch performance, MHD energy pumps operating at very high temperatures and hypersonic aerodynamics. Hossian and Takhar [1] presented radiation effects on mixed convection along a isothermal vertical plate. Bestman and Adjepong [2] studied the unsteady hydromagnetic free-convection flow with radiative hrat transfer in a rotating fluid. Raptis and Masslas [3] studied unsteady magnetohydrodynamic convection in a gray, absorbing but non-scatttering fluid regime using the Rosseland radiation model. Ganesan and Loganadan [4] presented Radiation and mass transfer effects on flow of an incompressible viscous fluid past a moving cylinder. Azzam [5] studied thermal radiation flux influence on hydromagnetic mixed free-forced convective steady optically-thick laminar boundary layer flow by using Rosseland approximation. Manca et. al [6] presented the effect on natural convection of the distance between an inclined discretely heated plate and a parallel shroud below. Abd-El-nay et. al [7] presented the radiation effects on MHD free convection flow over a vertical plate with variable surface temperature by finite difference solution. Muthucumaraswamy and Janakiraman [8] presented MHD and radiation effects on moving isothermal vertical plate with variable mass diffusion. Gbadeyan and idowu [9] studied the magnetohydrodynamic heat transfer between two concentric rotating spheres employing

* E-mail: prabhakar.bijjula@gmail.com

the optically thin limit case for thermal radiation. Heat and mass transfer of an unsteady MHD free convection flow of rotating fluid past a vertical porous flat plate in the presence of radiative heat transfer studied by Mbeledogu and Ogulu [10]. Shateyi et. al [11] presented numerical solutions for steady, laminar, magnetohydrodynamic convection flow past a semi-infinite vertical plate with thermal radiative heat transfer and Hall currents. Muthucumaraswamy et. al [12] studied unsteady flow past an accelerated infinite vertical plate with variable temperature and uniform mass diffusion. Mohamoud [13] presented temperature dependent viscosity effects in transient dissipative radiation hydrodynamic convection, showing that an increase in Eckert number and decrease in air viscosity accelerate the flow, whereas increasing magnetic field or thermal radiation flux decelerates the flow. Beg et. al [14] studied chemically-reacting mixed convective heat and mass transfer along inclined and vertical plates with Soret and Dufour effects. Anand Rao and Prabhakar Reddy [15] studied heat and mass transfer of an unsteady MHD natural convection flow over a rotating fluid past a vertical plate in the presence of radiative heat transfer by finite element method.

In this paper, we consider the unsteady gravity-driven thermal convection flow of a viscous incompressible, electrically-conducting, absorbing-emitting, optically-thick gray gas along an inclined plane in the presence of thermal radiation. The momentum and energy conservation equations are non-dimensionalzed and solved by using Ritz finite element method. The behaviors of the velocitiy, temperature, frictional shearing stress and wall temperature gradient have been discussed for variations in the governing parameters.

## 2. Mathematical Model

The transient hydro-magnetic flow of a viscous, incompressible, electrically conducting, absorbing-emitting, non-scattering, optically-thick gas along an infinite porous plate inclined at angle $a$ to the horizontal is considered. The plate moving with constant velocity $u_0$. Refractive index of the gas medium is constant. A uniform magnetic field$B_0$, applied normal to the plate. The $x'$-axis oriented along the plate and the $y'$ -axis perpendicular to the plate. The Maxwell field equations comprise five vector equations- the Ampere's law, magnetic field continuity, Faraday's law, Kirchoff's law and Ohm's law. The generalized equations in vector form, for flow of an electrically-conducting gas are the Maxwell equations:

$$\nabla \times B = \mu J \text{ Ampere's law} \tag{1}$$

$$\nabla \bullet B = 0 \text{ Magnetic Field Continuity (Maxwell Equation)} \tag{2}$$

$$\nabla \times E = -\frac{\partial B}{\partial t} \text{ Faraday's law} \tag{3}$$

$$\nabla \bullet J = 0 \text{ Kirchoff's law} \tag{4}$$

$$J = \sigma \left[E + v \times B\right] \text{ Ohm's law} \tag{5}$$

where $J$ is the current density, $B$ is the magnetic field vector, $\sigma$ is the electrical conductivity, $E$ is the electrical field density vector, $\rho$ is the density, $v$ is the velocity vector, $\mu$ is viscosity and $t$ is time. From an order of magnitude analysis, it can be shown that for two-dimensional $(xy)$ magneto-hydrodynamic gas dynamic flows, the hydromagnetic retarding force (Lorentz body force) acts only parallel to the flow and has the form:

$$F_{magnetic} \approx -\sigma B_y^2 u \tag{6}$$

where $B_y$ is the component of magnetic field in the $y-$direction. We consider an aerodynamic viscous flow where the magnetic field is sufficiently weak to sustain a small magnetic Reynolds number such that induced magnetic field effects can be neglected. Joule electro-heating and Hall current/ionslip effects are also neglected. The temperature of the gas in the regime is $T'$ and an induced pressure gradient generated by indirect natural convection acts along the $x'-$direction. All the fluid properties are constant; the plate temperature is prescribed $T_w{}'$ and is of sufficiently high magnitude that thermal radiation effects are significant. In accordance with the Boussinesq approximation, all fluid properties are constant with the exception of the density variation in the buoyancy term. Unidirectional radiation flux $Q_r$ is considered and it is assumed that$\frac{\partial Q_r}{\partial y'} >> \frac{\partial Q_r}{\partial x'}$. Under this assumptios, the mass, momentum and energy conservation equations for the regime with regard to indirect natural convection may be presented as follows.

$$\frac{\partial u'}{\partial x'} + \frac{\partial u'}{\partial y'} = 0 \tag{7}$$

$$\frac{\partial u'}{\partial t'} + u'\frac{\partial u'}{\partial x'} + v'\frac{\partial u'}{\partial y'} = -\frac{1}{\rho}\frac{\partial p}{\partial x'} + \nu\frac{\partial^2 u'}{\partial y'^2} - \frac{\sigma B_0^2 u'}{\rho} + g\beta\left(T' - T_\infty^{'}\right)\sin a - \frac{\nu u'}{K'} \tag{8}$$

$$0 = -\frac{1}{\rho}\frac{\partial p}{\partial x'} - g\beta\left(T' - T_\infty{}'\right)\cos a \tag{9}$$

$$\frac{\partial T'}{\partial t'} = \frac{k}{\rho C_p}\frac{\partial^2 T'}{\partial y'^2} - \frac{1}{\rho C_p}\frac{\partial Q_r}{\partial y'} \tag{10}$$

Subject to the following initial and boundary conditions:

$$t' \le 0 : u' = 0,\ T' = T_\infty{}' \text{ for all } y' \ge 0;\ t' > 0 : u' = u_0,\ T' = T_w \text{ for } y' = 0;\ u' \to 0,\ T' \to T_\infty{}' \text{ as } y' \to \infty \tag{11}$$

where $u'$ is the velocity in the $x'-$ direction, $v'$ is velocity in the $y'-$ direction, $g$ is acceleration due to gravity, $\nu$ is the kinematic viscosity of the optically-dense gas, $T'$ is temperature of the fluid, $T_\infty{}'$ is free stream temperature of the fluid, $T_w{}'$ is plate surface temperature, $\rho$ is the density, $C_p$ is specific heat at constant pressure, $k$ is thermal conductivity of the optically-dense fluid, $\beta$ is volumetric coefficient of thermal expansion, $t'$ is time, $B_0$ is uniform magnetic field, $\sigma$ is electrical conductivity of the gas and $Q_r$ is radiative heat flux.

In transient flow, the frictional (viscous) and gravitational forces do not balance exactly and the discrepancy is proportional to the acceleration of the fluid, the deviation between the free surface of the gas and the plate inclination also contributes to this and an instability mechanism arises in the inclined plane flow. There is pressure distribution in the flow with a gradient defined as:

$$\frac{\partial p}{\partial y'} = \rho g \tag{12}$$

From Equation (3), integration gives:

$$p = \rho g\beta\left(h - y'\right)\left(T' - T_\infty{}'\right)\cos a \tag{13}$$

where $h$ denotes free surface elevation. Differentiating Equation (13) with respect to $x'$ yields:

$$\frac{\partial p}{\partial x'} = \rho g\beta\left(T' - T_\infty^{'}\right)\frac{\partial h}{\partial x'}\cos a \tag{14}$$

Above the leading edge of the plate ($x' = 0$), the density variation with depth is constant i.e., will remains unchanged for all $\frac{\partial h}{\partial x'}$. We therefore prescribe the following condition:

$$\frac{\partial h}{\partial x'} = cons\tan t = F_1 \tag{15}$$

The following non-dimensional quantities introduced to transform equations (7) to (10) under the boundary conditions (11) into dimensionless form:

$$u = \frac{u'}{u_0}, y = \frac{u_0 y'}{\nu}, t = \frac{u_0^2 t'}{\nu}, \theta = \frac{T' - T_\infty{}'}{T_w{}' - T_\infty{}'}, P_r = \frac{\mu C_p}{k}, M = \frac{\sigma B_0^2 \nu}{\rho u_0^2}, \mu = \rho\upsilon, G_r = \frac{g\beta\nu(T_w - T_\infty)}{u_0^3} \tag{16}$$

where $u$ is dimensionless velocity in the $x'-$ direction, $t$ is non-dimensional time, $y$ is dimensionless transverse coordinate, $\theta$ is dimensionless temperature function, $G_r$ is the Grashof (free convection) number, $P_r$ is the Prandtl number and $M$ denotes the square root of the Hartmann hydro-magnetic number. Introducing the above non-dimensional variables into Equation (8) and (9) using Eq. (15) also, and neglecting convective acceleration terms, we get in due course at the dimensionless form of the momentum equation:

$$\frac{\partial u}{\partial t} = G_r (\sin a - F_1 \cos a)\, \theta + \frac{\partial^2 u}{\partial y^2} - M^2 u - \frac{u}{K} \tag{17}$$

The radiative heat flux vector is addressed using the Rosseland diffusion flux approximation is therefore used leading to a Fourier type gradient function viz:

$$Q_r = -\frac{4\sigma}{3k^*}\frac{\partial T'^4}{\partial y'} \tag{18}$$

where $\sigma$ is the Stefan-Boltzmann constant and $k^*$ is the spectral mean absorption coefficient of the medium. Considering the temperature differences within the flow sufficient small, $T'^4$can be expressed as the linear function of temperature $T'$. This is accomplished by expanding $T'^4$ in a Taylor series about a free stream temperature $T_\infty{}'$ and neglecting the higher-order terms,

$$T'^4 \cong 4T'^3_\infty T' - 3T'^4_\infty \tag{19}$$

By using Equations (16) and (19), Equation (10) reduces to

$$[1 + K_1]\frac{\partial^2 \theta}{\partial y^2} - P_r \frac{\partial \theta}{\partial t} = 0 \tag{20}$$

where $K_1 = \frac{16\sigma T'^3_\infty}{3k^\bullet k}$ denotes the Boltzmann-Rosseland radiation conduction number.

This parameter $K_1$ embodies the relative contribution of heat transfer by thermal radiation to thermal conduction; large $K_1$ $(> 1)$ corresponds to thermal radiation dominance and small $K_1$ $(< 1)$ to the thermal conduction dominance. For $K_1 = 1$ both conduction and radiative heat transfer modes contributes equally to the regime. Clearly the first term in Equation (20) is an augmented diffusion term i.e., with $K_1 = 0$, thermal radiation vanishes and Equation (20) reduces to the familiar unsteady one-dimensional conduction-convection equation. The boundary conditions Equation (11) are also transformed using (16) to:

$$t \le 0 : u = 0,\ \theta = 0 \text{ for } y \ge 0;\ t > 0 : u = 1,\ \theta = 1 \text{ for } y = 0;\ u \to 0,\ \theta \to 0 \text{ as } y \to \infty \tag{21}$$

## 3. Method of Solution

The governing equations (17) and (20) are to be solved under the initial and boundary conditions of equation (21). The Ritz finite element method is applied to solve these equations. The method entails the following steps.

(1). Division of the whole domain into smaller elements of finite dimensions called “finite elements”.

(2). Generation of the element equations using variational formulations.

(3). Assembly of element equations as obtained in step 2.

(4). Imposition of boundary conditions to the equations obtained in step 3.

(5). Solution of the assembled algebraic equations.

The assembled equations can be solved by any of the numerical technique viz. Gauss-seidal iteration method. Here, infinite is taken as $y = 10$. An important consideration is that of shape functions which are employed to approximate actual functions. For one dimensional and two dimensional problems, the shape factions can be linear/quadratic and higher order. However, the suitability of the shape functions varies from problem to problem. Due to simple and efficient use in computations linear shape functions are used in the present problem. To prove convergence and stability of the Ritz FEM, the computations are carried out by making small changes in time $t$ and $y-$directions. For these slightly changed values, no significant change was observed in the values of velocity $u$ and temperature $\theta$. Hence, the Ritz finite element method is convergent and stable. The frictional shearing stress at the plate surface ($y = 0$) and the wall temperature gradient are defined as:

$$\left(\frac{du}{dy}\right)_{y=0} \quad \text{and} \quad \left(\frac{d\theta}{dy}\right)_{y=0}$$

# 4. Numerical Results and Discussion

The problem of unsteady gravity-driven thermal convection flow of a viscous incompressible, electrically-conducting, absorbing-emitting, optically-thick gray gas along an inclined plane in the presence of thermal radiation is addressed in this study. The numerical calculation has been carried out for dimensionless velocity ($u$), temperature ($\theta$), Friction shearing stress and temperature gradient for various values of the material parameters. Numerical results are presented in figures and tables. These results show the effect of the material parameters on the quantities mentioned.

The effects of the Prandtl number $P_r$ on the velocity and temperature distributions with transverse coordinate ($y$) are shown in Figure 1 and 2, respectively. The numerical results show that the effect of increasing values of Prandtl number results in a decreasing velocity and temperature distributions. The effects of Boltzmann-Rosseland radiation convection parameter ($K_1$) on the velocity and temperature profiles are presented in Figure 3 and 4, respectively. It is seen that an increasing values of $K_1$ leads to increase in the velocity and temperature distributions. For $P_r = 0.71$ i.e., $P_r < 1$, heat diffuses faster than momentum in the regime. $K_1$ corresponds to an increase in the relative contribution of thermal radiation heat transfer to thermal conduction heat transfer.

As for $K_1 << 1$, thermal conduction heat transfer will dominate and vice versa for $K_1 > 1$. Larger values of $K_1$ therefore physically correspond to stronger thermal radiation flux and in accordance with this, the maximum temperature is observed for $K_1 = 3$ (Figure 4). Also, temperature profiles all decay monotonically from the maximum at the plate to the free stream. Figure 5 and 6 shows the velocity and temperature distributions with distance normal to the plate at various times ($t$) with $K_1 = 1.0$ (i.e., radiation and conduction contributions are equal).

It is observed that velocity and temperature distributions clearly increased in the regime with propagation of time. Also, observed that the decay in profiles tends to increasingly to a linear distribution with increasing time. The effects of Hartmann number square root ($M$) on the velocity distribution with distance normal to the plate ($y$) are presented in Figure 7. The hydromaggnetic term in Equation (17), i.e., $-M^2u$ is a linear drag force term. With increasing magnetic field strength $B_0$, $M$ is increased and this serves to decelerate the flow along the inclined plate. Also, observed that the velocity profiles are strongly reduced with increasing values of $M$. Further, we note that as $M$ rises, the velocity profiles decreases to zero progressively for shorter distance from the plate surface. Fig.8 depicts the effects of porosity parameter $K$ on the velocity distribution. It observed that an increasing value of porosity parameter increases the velocity profiles. The effects of free convection parameter i.e., Grashof number $G_r$ on the velocity distribution are presented in Figure 9.

It can be seen that an increase in the Grashof number leads to increase in the velocity. Free convection currents as simulated with the buoyancy term serve to accelerate the flow along the inclined plate. Figure 10 depicts the effects of plate inclination $(a)$ on the velocity distribution. It is observed that an increase in the plate inclination values increases the velocity profiles. A gradual decrease occurs from the plate to the free stream. Velocity becomes negative further from the plate surface for lower angle of inclination i.e., back flow arises. Also, we observe that an increase in angle of inclination to $45^0$, $60^0$ and to the maximum (vertical) orientation of $a = 90^0$, the flow is strongly accelerated.

The effects of $P_r$, $K_1$ and $t$ on the frictional shearing stress and plate temperature gradient are presented in Table 1. It is observed that an increase in the Prandtl number leads to decrease in both frictional shearing stress and plate temperature gradient. An increase in the Boltzmann-Rosseland radiation parameter and time parameter increases the frictional shearing stress and plate temperature gradient. The effects of $M$, $K$, $G_r$ and plate inclination $(a)$ on the frictional shearing stress are presented in Table 2. It can be seen that an increase in the square root of Hartmann number $(M)$ leads to decrease in the frictional shearing stress whereas an increase in the porosity parameter, Grashof number and plate inclination increases the frictional shearing stress. Here, increasing plate inclination serves to accelerate the flow and shearing stress magnitude strongly increased with rise in the Grashof number. Negative values indicate that back flow.

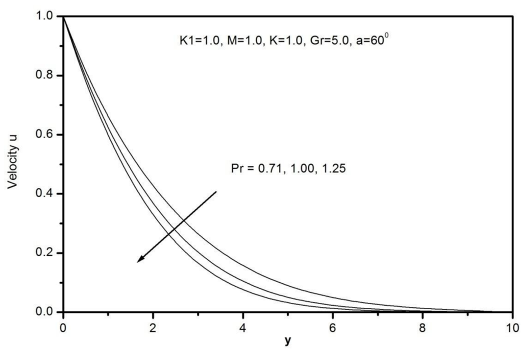


Figure 1: Velocity distribution for various values of $P_r$

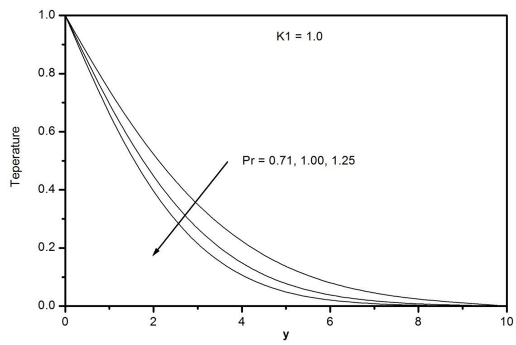


Figure 2: Temperature distribution for various values of $P_r$

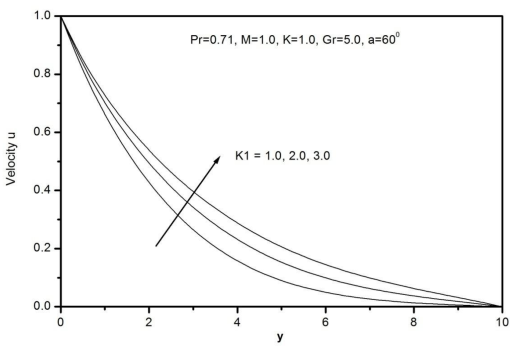


Figure 3: Velocity distribution for various values of $K_1$

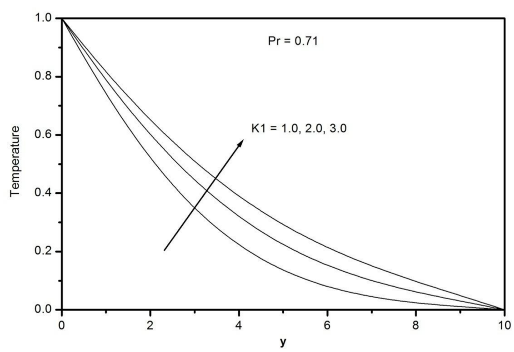


Figure 4: Temperature distribution for various values of $K_1$

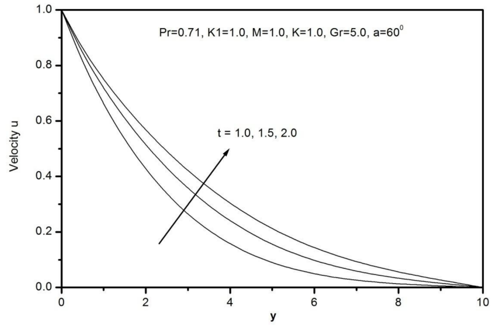


Figure 5: Velocity distribution for various values of time parameter $t$

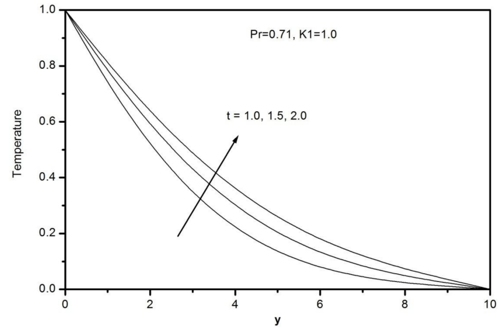


Figure 6: Temperature distribution for various values of time parameter $t$

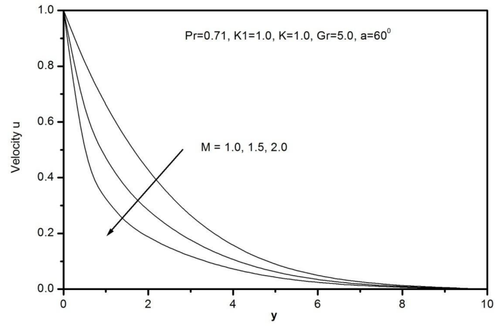


Figure 7: Velocity distribution for various values of $M$

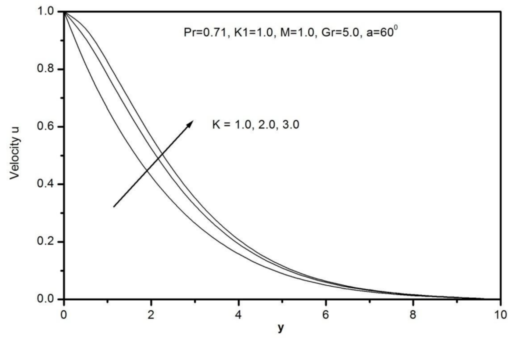


Figure 8: Velocity distribution for various values of $K$

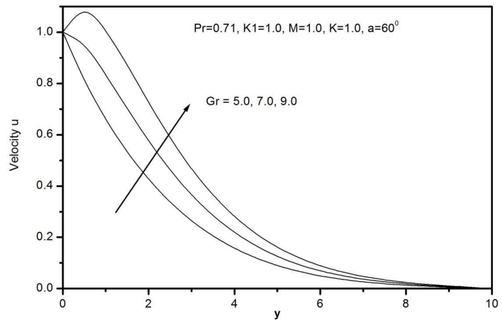


Figure 9: Velocity distribution for various values of $G_r$

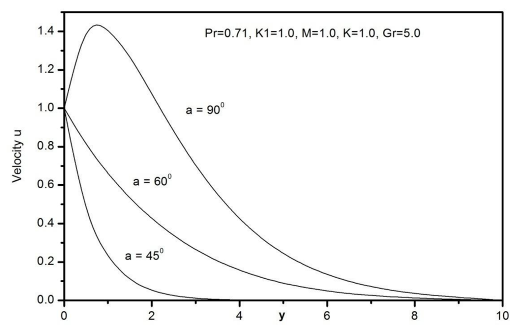


Figure 10: Velocity distribution for various inclinations of the plate $(a)$

| $P_r$ | $K_1$ | $t$ | $\left(\frac{du}{dy}\right)_{y=0}$ | $\left(\frac{d\theta}{dy}\right)_{y=0}$ |
|---|---|---|---|---|
| 0.71 | 1.0 | 1.0 | -0.370784 | -0.264320 |
| 1.00 | 1.0 | 1.0 | -0.410674 | -0.313596 |
| 0.71 | 2.0 | 1.0 | -0.328632 | -0.215644 |
| 0.71 | 1.0 | 2.0 | -0.274806 | -0.190394 |

Table 1: The numerical values of frictional shearing stress $\left(\frac{du}{dy}\right)_{y=0}$ and wall temperature gradient $\left(\frac{d\theta}{dy}\right)_{y=0}$ for various values of $P_r, K_1$ and time parameter $t$.

| $M$ | $K$ | $G_r$ | $a$(degrees) | $\left(\frac{du}{dy}\right)_{y=0}$ |
|---|---|---|---|---|
| 1.0 | 1.0 | 5.0 | 60 | -0.370784 |
| 2.0 | 1.0 | 5.0 | 60 | -0.984062 |
| 1.0 | 2.0 | 5.0 | 60 | -0.189678 |
| 1.0 | 1.0 | 7.0 | 90 | -0.106680 |
| 1.0 | 1.0 | 5.0 | 60 | 0.772824 |

Table 2: The numerical values of frictional shearing stress $\left(\frac{du}{dy}\right)_{y=0}$ for various values of $M, K, G_r$ & inclination of plate (a).

## 5. Conclusions

In this study we have examined the governing equations for unsteady gravity-driven thermal convection flow of a viscous incompressible, electrically-conducting, absorbing-emitting, optically-thick gray gas along an inclined plane in the presence of thermal radiation and a transverse magnetic field effects. The Rosseland diffusion flux model is employed to simulate thermal radiation effects. Employing the Ritz finite element method, the leading equations are solved numerically. We can conclude from these results that a decrease in the velocity and temperature occurs as the Prandtl number and Hartmann number square root are increased. The velocity and temperature increased as Boltzmann-Rosseland radiation parameter and Grashof number are increased. Also, an increase in the plate inclination values increases the velocity and the maximum (vertical) orientation of $a = 90°$, the flow is strongly accelerated (Figure 10).

## References


[1] M.A.Hossian and H.S.Takhar, *Radiation effects on mixed convection along a vertical plate with uniform surface temperature*, Int J Heat and Mass Transfer, 31(1996), 243-248.

[2] A.R.Bestman and S.K.Adjepong, *Unsteady hydromagnetic free-convection flow with radiative hrat transfer in a rotating fluid*, Astrophysics Space Sciene, 143(1998), 217-224.

[3] A.Raptis and C.V.Masslas, *Magnetohydrodynamic flow past a plate by the presence of radiation*, Heat and Mass Transfer, 34(1998), 107-109.

[4] P.Ganesan and P.Loganadan, *Radiation and mass transfer effects on flow of an incompressible viscous fluid past a moving cylinder*, Int J Heat and Mass Transfer, 45(2002), 4281-4288.

[5] G.Azzam, *Radiation effects on the MHD mixed free-forced convective flow past a semi-infinite moving vertical plate for high temperature differences*, Physica Scripta, 66(2002), 71-76.

[6] O.Manca, S.Nardini and V.Naso, *Effect on natural convection of the distance between an inclined discretely heated plate and a parallel shroud below*, ASME Journal of Heat Transfer, 124(2002), 441-450.

[7] M.A.Abd-El-Nay, M.E.Elasayed, Elbarbary, Nadar and Abdelzem, *Finite difference solution of radiation effects on MHD free convection flow over a vertical plate with variable surface temperature*, J. Appl. Maths., 2(2003), 65-86.

[8] R.Muthucumaraswamy and B.Janakiraman, *MHD and radiation effects on moving isothermal vertical plate with variable mass diffusion*, Theoret Appl Mech, 33(2006), 17-29.

[9] J.A.Gbadeyan and A.S.Idowu, *Radiation effects on magnetohydrodynamic flow of gas between two concentric spheres*, Journal of the Nigerian Association of Mathematical Physics, 10(2006), 305-314.

[10] I.U.Mbeledogu and A.Ogulu, *Heat and mass transfer of an unsteady MHD free convection flow of rotating fluid past a vertical porous flat plate in the presence of radiative heat transfer*, Int. J. heat and Mass Transfer, 50(2007), 1902-1908.

[11] S.Shateyi, P.Sibanda and S.S.Motsa, *Magneto-hydrodynamic flow past a vertical plate with radiativr heat transfer*, ASME Journal of Heat Transfer, 129(2007), 1708-1712.

[12] R.Muthucumaraswamy, M.Sunder Raj and V.S.A.Subramanian, *Unsteady flow past an accelerated infinite vertical plate with variable temperature and uniform mass diffusion*, Int. J. Appl. Math and Mech., 5(6)(2009), 51-56.

[13] M.A.A.Mohamoud, *Thermal radiation effect on unsteady MHD free convection flow past a vertical plate with temperature dependent viscosity*, Canadian Journal of Chemical Engineering, 87(2009), 441-450.

[14] O.Beg, Anwar, T.A.Beg, A.Y.Bakier and V.R.Prasad, *Chemically-reacting mixed convective heat and mass transfer along inclined and vertical plates with Soret and Dufour effects: Numerical solutions*, Int. J. Appl. Math and Mech., 5(2009), 39-57.

[15] J.Anand Rao and B.Prabhakar Reddy, *Finite element analysis of heat and mass transfer of an unsteady MHD natural convection flow of a rotating fluid past a vertical porous plate in the presence of radiative heat transfer*, 32(2010), 223-241.